The dynamics of NH_4^+ in the NH_4MF_3 perovskites. II. Inelastic neutron scattering study

1995 J. Phys.: Condens. Matter 7 8723

(http://iopscience.iop.org/0953-8984/7/46/005)

J. Phys.: Condens. Matter 7 (1995) 8723–8740. Printed in the UK

The dynamics of NH_4^+ in the NH_4MF_3 perovskites: II. Inelastic neutron scattering study

J Rubín†‡, J Bartolomé† and J Tomkinson§

† Instituto de Ciencia de Materiales de Aragón, CSIC—Universidad de Zaragoza, 50009 Zaragoza, Spain

‡ Departamento de Física de la Materia Condensada, Universidad de Zaragoza, 50009 Zaragoza, Spain

§ ISIS Facility, Rutherford Appleton Laboratory, Chilton, Oxfordshire, UK

Received 24 March 1995, in final form 11 July 1995

Abstract. Inelastic neutron scattering experiments have been performed to study the librational motion of the NH_4^+ ion in the perovskite family NH_4MF_3 (M = Zn, Mn and Cd). The first excited librational band appears as a broad peak in the high-temperature cubic phase. Below the structural phase transition, to a lower symmetry, the band splits into three narrow features. The overtone bands are also detected in the Cd compound. The frequencies of the fundamentals increase for increasing cell size (Zn > Mn > Cd), the same trend as the activation energies. The INS spectra are analysed quantitatively by expanding the potential in symmetry adapted rotational wavefunctions.

1. Introduction

The dynamics of the molecular group NH_4^+ in solids is determined by the interaction with the field produced by surrounding atoms or ions. As recalled in the introduction of the previous paper (Rubín *et al* 1994, paper I of this series), the experimental study of the different kinds of motion of the ion provides information about the field strengths and symmetry properties. This study of the interaction of the rotator NH_4^+ in the ammonium perovskites aims to understand and parametrize the ion's rotational potential field. The potential field of NH_4MnF_3 has already been parametrized in the high-temperature phase from diffraction results (Rubín *et al* 1995b). In low-temperature phase this analysis fails due to the high localization of the hydrogen atoms (Press and Hüller 1973) and the spectroscopic alternative, inelastic neutron scattering (INS), is used.

Paper I reported the quasielastic neutron scattering study of the ammonium ion rotations in the fluoroperovskite family NH_4MF_3 (M = Mg, Zn, Mn and Cd). These compounds exhibit a perovskite structure, cubic in the high-temperature phase, and distorted to orthorhombic in the low-temperature phase. This structural transition involves a change in the environment of the ammonium ion and therefore in its dynamics. The activation energies, E_a, of the rotational jump processes were measured in both structural phases. In the high-temperature phase the trend was of an increasing E_a with increasing cell parameters which parallels observations reported for the low-temperature phase (Palacios *et al* 1989). These trends are opposite to the prediction provided by a model in which only electrostatic interactions are considered (Bartolomé *et al* 1977, Smith 1987).

0953-8984/95/468723+18$19.50

The measurement of the elastic incoherent structure factor (EISF) demonstrated the existence of a preferential axis for the reorientation of the NH_4^+, in the high-temperature phase. This axis is determined by the orientation of the ammonium tetrahedron in the cubic cage. It was concluded that the main rotational process consists of 180° jumps about the preferential axis and there is predominantly one orientation of the NH_4^+ ion. Other 180° jumps about axes perpendicular to the preferential axis were also observed, and these drive the molecule to other orientations. It was also concluded that the classical path for the rotations is probably that of 120° rotations about threefold ammonium axes. Two such rotations about different axes would appear as a single 180° jump.

However, in the orthorhombic low-temperature phase of the Mn salt this model could not explain the EISF. Instead an asymmetric double-well potential was used. The ammonium ion was thought to jump between the low-energy well and the other, high-energy well, corresponding to a different orientation. The calculated jump distances in this double-well model were consistent with 180° rotations around a twofold axis of the ammonium ion. When the sample is slightly below the transition temperature the trajectory of the NH_4^+ jumps constitutes a special limit. These are limiting case jumps and correspond to 180° jumps exclusively about the preferential axis.

In this paper we report the librational INS spectrum of the NH_4^+ ion in the fluoroperovskites. In both structural phases a comparison of the observed spectra with the calculated spectra is presented. The temperature dependence of the Raman spectrum will be reported elsewhere (Rubín *et al* 1995a).

2. Experimental results

The TFXA spectrometer at the ISIS Facility, Rutherford Appleton Laboratory, UK, was used. This is an inverted geometry spectrometer where a white incident neutron beam illuminates the sample and undergoes Stokes scattering. The fixed final neutron energy is determined by a crystal analyser in a special time focusing arrangement. Further details are provided elsewhere (Penfold and Tomkinson 1986). The energy transfer, E_t, covers the range from 2 to 500 meV, with a Gaussian shaped energy resolution of $\Delta E_t/E_t \approx 2\%$. The spectra are collected at a fixed scattering angle of 133°, and the momentum transfers (in $Å^{-1}$), Q, are approximately given by $Q^2 = E_t/2$. TFXA is well suited to the study of molecular librations in low-temperature solids. The samples were powders and the experimental spectra were corrected for background scattering from the cryostat.

The INS spectrum of NH_4^+ was obtained in the Mn and Zn perovskites in both structural phases, and in the Cd salt in the low-temperature phase. In figures 1 and 2 these spectra are shown for energy transfers up to 150 meV. Above these energies other peaks appear but these correspond to the internal modes of the molecular ion and are not discussed here.

2.1. *The low-temperature phase*

It is convenient to separate the INS spectra into three energy regions.

(a) *The region below ~30 meV.* This shows a spectrum of low intensity and is normally associated with the translational phonon density of states.

(b) *The region from ~30 to ~60 meV.* This shows three features whose intensity is consistent with a conventional assignment to librations. These are the librations that will be the main theme of our discussions below. The intensity of these features arises in the main from the high incoherent scattering cross-section of hydrogen (80 barn) and the large

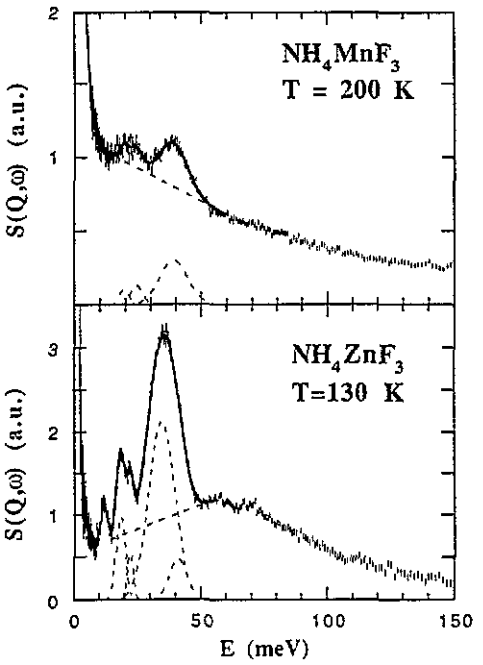

Figure 1. Inelastic neutron scattering spectra of NH_4ZnF_3 and NH_4MnF_3 in the high-temperature phase. The full line is the fit to the experimental data using several Gaussian components, drawn in broken lines. The straight slope in the broken line is the base line used in the fits, but does not necessarily represent the real background of the scattering intensity of the librational modes.

amplitudes associated with librational displacements.

(c) *The region above ~60 meV.* This shows weak but well defined features in the Cd salt and a broad band in the Mn and Zn salts.

2.2. *The high-temperature phase*

All the spectroscopic structure in the (b) region has disappeared. In the Mn salt the main feature of the spectrum is an intense broad peak centred at ~ 39 meV, whilst the Zn salt spectrum shows two very broad features centred at ~ 34 and 60 meV.

The bands have an approximately Gaussian shape and their positions, full widths at half height (FWHHs), and intensities were extracted by a Gaussian fitting program. For the Zn salt in the high-temperature phase, the band is slightly asymmetric, and a small Gaussian component is added to the main feature centred at 34.4 meV. As can be seen in figures 1 and 2 the librational bands contain a non-constant background which is approximated by a slope. It is unclear to what extent this contains librational mode intensity. It is likely that two phonon events from the phonon density of states are responsible for much of this intensity. The results of the fittings are reported in table 1. The FWHHs in table 1 correspond to the fitting Gaussians (upon the slope). This is important in the Zn salt high-temperature phase, since the fitted Gaussian has FWHH = 12 meV, while the total experimental feature in the spectrum (no slope background subtracted) has FWHH = 16 meV.

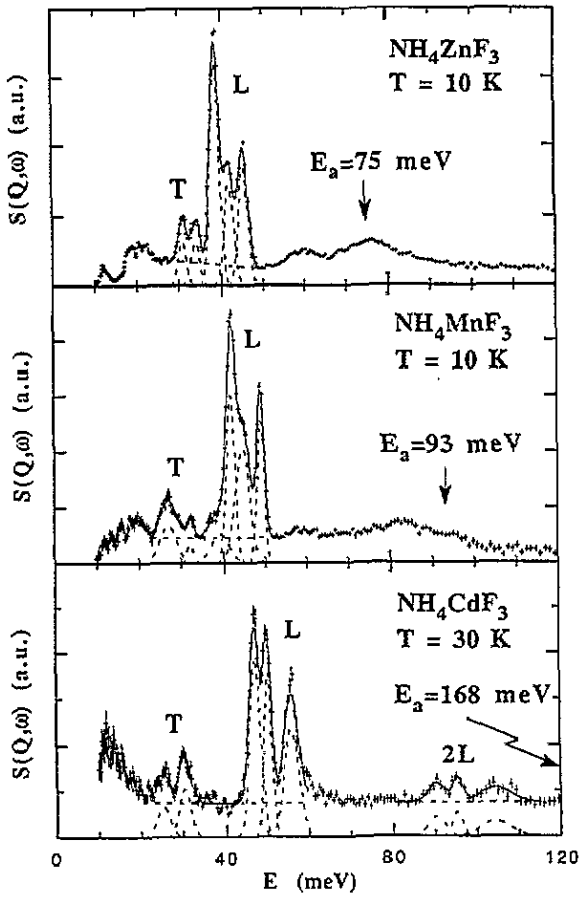

Figure 2. Inelastic neutron scattering spectra of NH_4ZnF_3, NH_4MnF_3 and NH_4CdF_3 in the low-temperature phase. The full line is the fit to the experimental data using several Gaussian components, drawn in broken lines. The peaks assigned to librational modes are denoted by L, while those assigned to translational modes are denoted by T. In NH_4CdF_3, more librational modes appear at higher energies and they are marked by 2L. The activation energies, E_a, are also indicated.

3. The librational energy spectrum and the neutron scattering function

The neutron incoherent scattering function for the rotational transitions from the rotational ground state of the ammonium ion can be written in terms of a normalized density of states, $Z_R(\omega)$, as

$$S_1^A(Q,\omega) = \frac{1}{\hbar^2}\frac{\sigma_{inc}}{4\pi}\exp[-2W(Q)]\frac{\hbar^2Q^2}{2M}\frac{Z_R(\omega)}{\omega}[n(\omega)+1] \tag{1}$$

$$Z_R(\omega) = \sum_{i=1}^{N} g_i\delta(\omega - E_i/\hbar)$$

where M is the effective mass of the molecule ($M = 4m$ for rotational motions), E_i and g_i are the rotational levels and degeneracies, σ_{inc} is the incoherent cross-sections of hydrogen, $n(\omega)$ is the thermal population number, Q is the momentum transfer and $W(Q) = U^2Q^2$ is the Debye–Waller factor for mean square displacement U^2.

Table 1. Fitted positions and widths of the neutron scattering spectra of NH_4ZnF_3, NH_4MnF_3 and NH_4CdF_3 in the high-temperature and low-temperature phases. E_{Li} stands for the centres of the peaks assigned to librational modes of the NH_4^+ ion, while E_{Ti} stands for the centres of the peaks assigned to translational modes. FWHH are full widths at half height. The standard deviations of the parameters fitted are in brackets. All quantities are in meV.

	NH_4ZnF_3	NH_4MnF_3	NH_4CdF_3
High-temperature phase			
E_L	34.4(7)	39.1(2)	—
$FWHH_L$	12.0(8)	13.0(4)	—
Low-temperature phase			
E_{T1}	30.97(3)	27.1(1)	25.3(2)
$FWHH_{T1}$	2.2(2)	4.7(3)	3.6(7)
E_{T2}	33.97(3)	32.3(1)	30.4(2)
$FWHH_{T2}$	2.3(2)	1.6(3)	3.1(3)
E_{L1}	38.71(2)	41.76(8)	47.1(1)
$FWHH_{L1}$	2.53(7)	2.3(2)	3.0(2)
E_{L2}	42.00(3)	44.5(3)	50.2(1)
$FWHH_{L2}$	2.6(2)	4.0(6)	2.1(2)
E_{L3}	45.47(2)	49.00(4)	55.81(9)
$FWHH_{L3}$	2.6(1)	2.01(7)	4.1(2)
E_{L4}	—	—	90.3(4)
$FWHH_{L4}$	—	—	3.8(9)
E_{L5}	—	—	95.3(3)
$FWHH_{L5}$	—	—	2.7(6)
E_{L6}	—	—	104.3(5)
$FWHH_{L6}$	—	—	8.4(13)

Expression (1) calculates the full librational spectrum, using E_i and g_i obtained from the potential energy function for angular displacements with the molecular centre of mass fixed. Here it is assumed that the external, whole-body librations of an ion with stiff covalent bonds can be separated from those of the other atoms (Venkataraman and Sahni 1970). The interaction potential of the ion with its environment consists of a time-independent (static) part and a time-dependent part. The static part, $V(\Omega)$, contains the potential field of the ion in the (time average) charge distributions of the surrounding lattice. The potential $V(\Omega)$ must demonstrate the symmetry properties of the product group G of the crystalline space group, S, and molecular point group, M, as in $G = M \times S$ (King and Hornig 1966).

The space group of the cubic perovskite is $Pm3m$ with the tetrahedral ammonium ion, T_d, located on an octahedral site, O_h. Thus $V(\Omega)$ has to be constructed with the symmetry $T_d \times O_h$. Because both groups contain improper rotations the potential function must have the symmetry of the direct group constructed with two groups which are isomorphic with the smallest proper groups which contain all the proper rotations of the corresponding M and S groups (Miller and Decius 1973). We will call these groups Q_p groups. In particular, if there is a centre of symmetry Q_p is isomorphic with the subgroup (of M or S) which contains all the proper rotations. Since T_d contains no centre of symmetry its Q_p group

is the group O. Because O_h has a centre of symmetry its Q_p group is also the group O. Consequently the full symmetry of the potential function $V(\Omega)$ is $O \times O$ and it is given by an expansion in symmetry adapted functions SAFs (King and Hornig 1966),

$$V(\Omega) = B\beta \sum_{J,n} \beta_{J,n}(r) V_{J,n}(\Omega) \tag{2}$$

where Ω are the Euler angles that relate the ionic orientation to the crystal frame, $B = \hbar^2/(2I)$, I is the ion's moment of inertia, $V_{J,n}$ are the SAFs (which can be obtained from Altmann and Cracknell (1965) and Bradley and Cracknell (1972)), the index J is the total angular momentum and n is an index for multiple representations in a given value of J. The values of the coefficients β and $\beta_{J,n}$ depend on the distances between atoms. At the equilibrium positions β controls the strength of the interaction (actually the product $B\beta$) and the coefficients $\beta_{J,n}$ determine the orientation of the molecule in the crystal frame.

The expansion (2) is especially useful since it can be truncated to its leading terms and yet remains accurate. This is possible because (2) is the multipolar expansion of the interaction potential of the charge distribution of the NH_4^+. The octopolar term is the first non-zero multipolar moment. Calculations of the energy spectrum obtained from a Hamiltonian with the potential energy (2) require a set of wavefunctions. These are symmetry adapted linear combinations of the free rotor wavefunctions (Altmann and Cracknell 1965). In practice a finite set of wavefunctions is taken to a particular value of angular momentum, L, chosen so as to achieve energy convergence. This value of L increases as the librational energies increase.

When the crystal potential is large or the temperature is very low, the potential well becomes relatively deep. In the limit of a truly deep well the molecular motion is approximated to that of separable harmonic oscillators where some (or all) of the symmetry operations of the crystal group become quenched (Miller and Decius 1973), e.g. those that produce a reorientation of the molecule with respect to the crystal frame. In such circumstances only the common symmetry operations of both groups are effective, and the new effective point group is $E = S \cap M$. As a consequence of the particular orientation of the ammonium ion in the cubic crystal cage of the fluoroperovskites $E = D_{2d}$ (Helmholdt *et al* 1980, Rubín *et al* 1995b).

Expression (2) is purely static and so takes no account of interactions of the molecule with the time-dependent (phonon) part of the potential. It is just such interactions that could lead to line broadening effects. Four line broadening mechanisms can be identified: first, a libration–phonon coupling; second, instrumental resolution effects; third, tunnelling; and fourth, dispersion. Libration–phonon coupling links the librational potential field to the phonon density of states and leads to short, usually final state, lifetimes. This will be discussed further, below and elsewhere (Rubín *et al* 1995a). The instrumental resolution makes no significant contribution to our observed band widths, nevertheless we have explicitly included these effects in our calculations. In high-symmetry lattices the ammonium ion is often found to tunnel. This raises the natural degeneracy of the librational levels by only small energies and leads to bands of librational states. Though searched by NMR (Palacios *et al* 1989), there is no evidence for tunnelling in these systems and this mechanism is rejected. Dispersion of the librational modes, due to ammonium–ammonium coupling, has been suggested for other ammonium salts (NH_4Br (Goyal *et al* 1987); $(NH_4)_2SnCl_6$ (Prager *et al* 1977)). However experiments carried out specifically to observe this effect have underlined the single-particle character of the librational modes (Teh and Brockhouse 1971, Powell *et al* 1985).

4. The librational energy spectrum in the high-temperature phase

The INS spectrum of the Zn salt in the high-temperature, cubic, phase is shown in figure 1 and detailed in table 1. Only one intense, broad, feature is observed, at 34.4 meV. We shall now proceed to analyse this simple intensity distribution with the full spectrum of the librational states obtained from SAF. In the cubic perovskites, as discussed above, most of the terms in (2) cancel by symmetry and truncating terms $J > 6$ (Bartolomé *et al* 1977) leads to

$$V(\Omega) = B\beta(\beta_4 V_4(\Omega) + \beta_6 V_6(\Omega)) \qquad (3)$$
$$\beta_4^2 + \beta_6^2 = 1$$

where the normalization condition is imposed by the truncation. For O × O symmetry the next non-zero term in (2) is V_8, since V_7 cancels. The values of β_4 and β_6 mimic the shape of the potential function. For the ammonium perovskites, with the ammonium ion at the centre of the cubic cage and the positive ions at the corners, β_4 has to be negative (Bartolomé *et al* 1977, Ozaki *et al* 1985). The validity of the truncation at $J = 6$ depends on the convergence of the calculated librational energies. Satisfactory convergence is achieved for $L = 16$ for the ground and first excited states (King and Hornig 1966, Bartolomé *et al* 1977). For the Zn salt the previously published values $\beta = 40$, $\beta_4 = -0.250$ and $\beta_6 = 0.968$ were used in the potential function (3). (An effective charge of 0.42 e^+ on the hydrogen atoms was used and the rotational constant of the ammonium ion was $B = 8.48$ K, which corresponds to an N–H bond length of 1.033 Å.) These values predict a single librational band centred at 31 meV. This compares favourably with the experimental observation of 34.4 meV.

We intended to parametrize the potential as written in (3) to obtain an acceptable resemblance of the experimental spectrum. Therefore the parameters β, β_4 and β_6 were adjusted, starting from the values of Bartolomé *et al* (1977). The best agreement was obtained with $\beta = 50$, $\beta_4 = -0.28$ and $\beta_6 = 0.96$ (this value of β corresponds to allowing the effective hydrogen charge to vary up to 0.53 e^+). It was verified that the position of the band centre was insensitive to variations of β_4 or β_6 by less than 3%. These values were used to obtain the rotational level scheme, as a function of β, shown in figure 3 and the corresponding INS spectrum was calculated using Gaussian band shapes and is shown in figure 4 as a broken line. This calculation only included the spectrometer resolution broadening effects. The calculated spectrum predicts the position of the main peak at ≈ 34 meV correctly and also shows that the intensity around 60 meV involves librations and thus it is not exclusively due to multiphonon scattering. However, as can be seen from the figure the shape of the librational band is poorly simulated. The calculation was repeated using Lorentzian band shapes (FWHH = 14 meV) and the mean square displacement of the hydrogen atoms $U^2 = 0.063$ Å^2. A better fit was obtained (full line in figure 4). However, neglecting multiphonon scattering overestimates the librational contribution, and this can produce underestimation of the Debye–Waller factor.

The librational transitions in the cubic phase of the Zn salt have been published previously (Smith 1987). However, there are several differences between our calculations and those of Smith (1987) which must be appreciated before the results can be compared. First, the previous work included the third term in the expansion of the potential function, $\beta_8 V_8(\Omega)$; second, librational energies were only calculated in the deep well (harmonic approximation); third, the parameters β_i were calculated for an explicit form of the interaction and atomic arrangement in which the electrostatic interaction was proportional to the effective hydrogen charge; fourth, polarization and repulsion terms were included; fifth, only next neighbours were included (i.e. monopole–octopole interactions between a

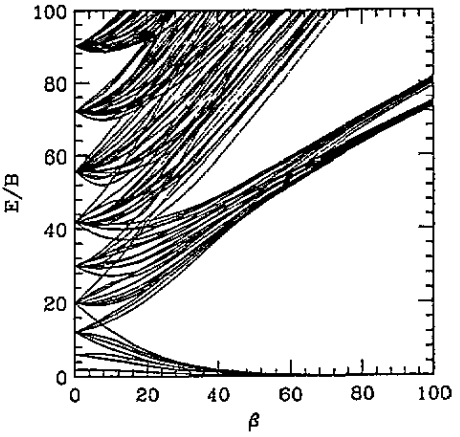

Figure 3. Librational energy level scheme corresponding to a tetrahedral rotor in a cubic potential represented by $V(\Omega) = \beta B\{\beta_4 V_4(\Omega) + \beta_6 V(\Omega)\}$ with $\beta_4 = -0.28$ and $\beta_6 = 0.96$, calculated as a function of β. The energies are shown in units of the rotational constant B.

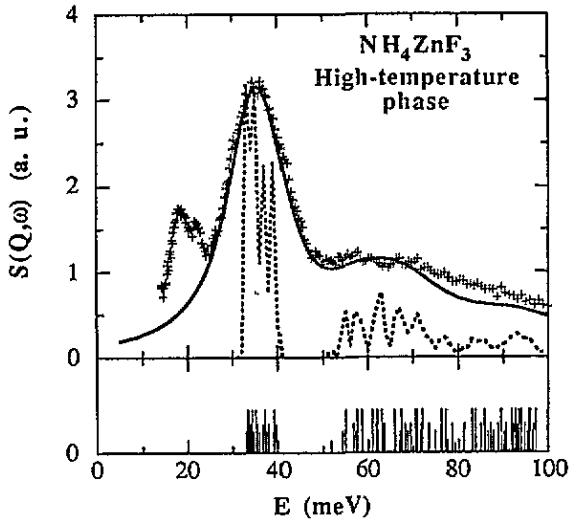

Figure 4. Simulation of the INS spectrum of the NH_4^+ rotor in NH_4ZnF_3 in the high-temperature phase using the calculated energy level scheme shown in figure 3 for $\beta = 50$ and $B = 8.48$ K. Broken line: simulated spectrum where only the resolution broadening is taken into account. Full line: simulated spectrum where each librational level is given a full width at half height of 12 meV in addition to the resolution broadening. In the lower part of the figure, energy level scheme with their relative degeneracy represented by the length of the bars.

particular NH_4^+ and a neighbouring NH_4^+ group were ignored). This latter is particularly disturbing since this distance, 4.2 Å, is similar to the ammonium–metal distance, 3.6 Å. The published parameters at 130 K were $\beta = 33.5$, $\beta_4 = -0.063$, $\beta_6 = 0.997$ and $\beta_8 = 0.055$. The effective hydrogen charge was fixed at $f = 0.19e^+$. The strength of the polarization term was adjusted to obtain the experimental librational energies and activation energies known at that time. This calculation is unable to yield the experimentally observed trend in E_a correctly. This failure is probably due to considering the effective charge, f, as a fixed

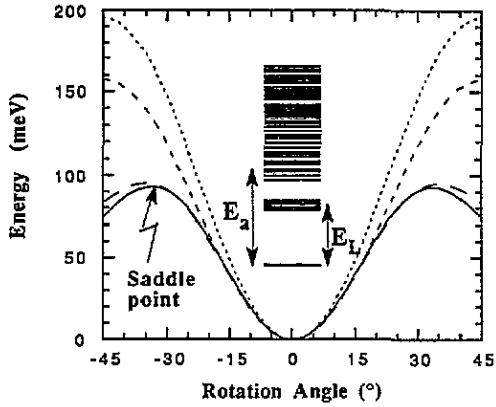

Figure 5. Potential energy barriers calculated from expression (2) (high-temperature phase) for $\beta = 50$, $\beta_4 = -0.28$ and $\beta_6 = 0.96$ (case of NH_4ZnF_3) and various axes for rotations of the NH_4^+ group. The librational energy levels are shown only up to 160 meV (energy with respect to zero potential energy) and E_a is taken from Brom and Bartolomé (1981). The line codes are as follows. Dots: rotation around the preferential axis. Short dashed: an axis perpendicular to the preferential axis. Long dashed: a threefold axis of the NH_4^+ tetrahedron. Full: a twofold axis of the perovskite structure which is close to a threefold axis of the NH_4^+ tetrahedron.

parameter for the whole series of compounds.

The calculated potential field also provides an estimate of the E_a. This is obtained by calculating the fields as the NH_4^+ ion is rotated about differently oriented axes and finding the lowest barrier in the potential energy surface. This is a saddle point and is sketched in figure 5. This saddle point represents the barrier to 120° jumps of the ion about non-preferential axes. This calculation supports our earlier suggestion that NH_4^+ reorientation involves double 120° jumps about the non-preferential axes (Rubín *et al* 1994). The barrier to rotation about the preferential axes is about twice as high. The relevant rôle of double jumps has already been shown in NH_4Cl (Gerling and Hüller 1983). Also shown in figure 5 are the energy levels; the librational transitions are labelled E_L. Those levels above the saddle point energy represent a quasicontinuum and are responsible for the reorientational motions of the ammonium ion. These are still bound states and in the deep-well approximation would be described as the overtones, but the anharmonic corrections are now so severe that this description looses utility. Transitions to these levels remain INS active and should appear as a broad undifferentiated feature beginning at about the value of E_a. In our spectrum a broad band does occur at about 54 meV. This compares favourably with the E_a values in the literature: NMR, 58.6 meV (Brom and Bartolomé 1981) and quasielastic neutron scattering, 50 meV (Steenbergen *et al* 1979).

We will now consider the band broadening processes. As discussed above only libration–phonon coupling provides a realistic mechanism for broadening our bands. The magnitude of the effect can be judged by eliminating the other contributions. These are the intrinsic width of the ground state, about 1 meV, and the instrumental resolution, about 0.7 meV. Therefore the result of lifetime effects is approximately 12 meV out of the 14 meV width used in the calculations of the INS intensity. We estimate that the minimum lifetime of the excited states is 0.1 ps. From the QNS measurements of Steenbergen *et al* (1979) the residence time of the ammonium ion in a particular orientation can be extrapolated at 130 K, yielding a value of 5 ps. If we associate this with the ground state lifetime then the

excited states collapse after a life 50 times shorter. We believe that this is the first clear-cut observation of lifetime broadening in the INS of librations. Other ammonium salts have given broad spectra but these were associated with unresolved splittings ($(NH_4)_2PdCl_6$ and $(NH_4)_2TeCl_6$ (Otnes and Svare 1979)) or with tunnel broadened ground states ($(NH_4)_2SnCl_6$ (Prager *et al* 1977)).

The procedures used above to analyse the Zn salt INS spectrum should be used in the case of the Mn salt. Unfortunately, because of the high temperature (T_c = 182 K), the librational signal is weak and the underlying slope is very intense. Only the band position can be extracted with confidence. This is 39 meV and corresponds to a β value of ≈ 54. From the diffraction parameters (B = 9.11 K, which corresponds to a N–H distance of 0.997 Å (Rubín *et al* 1995b)) $\beta_6 = 0.963$ and this gives $\beta = 50$. Alternatively, using $B = 9.11$ K for the Zn salt, $\beta = 47$. All of these values are tabulated in table 2.

Table 2. Parameters of the potential energy function for the high-temperature and low-temperature phases of NH_4ZnF_3, NH_4MnF_3 and NH_4CdF_3. In all the calculations the rotational constant has been taken as B = 8.48 K.

	NH_4ZnF_3	NH_4MnF_3	NH_4CdF_3
High-temperature phase			
β	50	54[a]	—
β_4	−0.28	−0.27[b]	—
β_6	0.96	0.963[b]	—
Low-temperature phase			
β	59	66[c]	75[c]
β_{41}	−0.1800	−0.2062	−0.2062
β_{42}	0	0	0
β_{43}	−0.153	−0.1742	−0.1742
β_{61}	0.3440	0.3404	0.3340
β_{62}	0	0.0200	0.0500
β_{63}	−0.908 77	−0.900 32	−0.897 15
β_{64}	0	0	−0.0200

[a] For NH_4MnF_3 (Rubín *et al* 1995b) the rotational constant has been measured (B = 9.11 K), which modifies the parameter β to 50.

[b] Values from Rubín *et al* (1995b).

[c] The starting values of the parameters $\beta_{J,n}$ were taken from those of the high-temperature phase of NH_4MnF_3.

5. The librational energy spectrum in the low-temperature phase

5.1. Assignment of librational and translational bands in the low-temperature phase spectrum

The INS spectra of the salts are shown in figure 2 and tabulated in table 1. A visual comparison of the spectra in figures 2 and 6 shows two important groups. The first, and most obvious, is a group of three intense lines that consistently move to high energies as the lattice parameter increases. These are the librational transitions and are labelled L in figures 2 and 6. The second group of lines is much weaker, and more complex. In the Zn salt it consists of two narrow lines; in the Mn salt it is one broad and one narrow line; finally in the Cd salt it becomes two broad lines. This group consistently moves down in energy as the lattice parameter increases. These are the translational transitions, and are

labelled T in figure 6. The shift to lower energies as the lattice expands is consistent with the same trend observed in optical phonon modes by Raman spectroscopy (Bartolomé *et al* 1985).

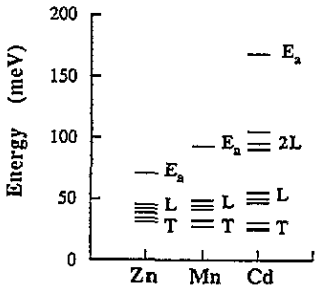

Figure 6. Representation of the centres of the peaks of the INS spectra in the low-temperature phase with their assignment. L: librational modes, T: translational modes. The activation energies, E_a, are also indicated. The cell parameters of these perovskites increase in the sequence Zn, Mn, Cd.

The presence of three sharp librational modes is consistent with a well defined low-symmetry potential and, indeed, an effective symmetry of C_s has been proposed for the NH_4^+ in the Zn salt (Knop *et al* 1981, Agulló-Rueda *et al* 1988). This has been confirmed specifically for the librational bands by Raman spectroscopy (Laguna *et al* 1993). The movement of the librational transitions to higher energies as the lattice expands is related to a similar trend in E_a values. The mean librational energies of the salts, see table 1, rank as Zn (42.1 meV) < Mn (45.1 meV) < Cd (51.0 meV) and the E_a values as Zn (75 meV) < Mn (93 meV) < Cd (168 meV) (Rubín *et al* 1994). We believe that this is due to shortening bonds between the ammonium ion and the closest fluorine atoms. Where the crystal structures are known this shortening has been verified; in the Mn salt the N–F distance is 2.84 Å (Rubín *et al* 1995b) and in the Cd salt it is 2.76 Å (Le Bail *et al* 1990). The increased electrostatic attraction will readily account for a deeper potential and provides pleasing support for our assignment scheme.

Above the librational features in the Zn and Mn salts very broad, low-intensity bands appear. In the deep-well approximation these bands would correspond to overtones and combinations of the librational modes. However the relatively low E_a values in the Zn and Mn salts suggest that the description in terms of transitions to a quasicontinuum may be better for these spectra. (This was discussed above for the case of the Zn salt.) Only the Cd salt spectrum can be safely described in the deep-well approximation and we proceed to do this below.

5.2. Higher harmonics of the librational modes of the Cd salt

In the Cd salt spectrum the three peaks around 100 meV are well defined, see figure 2. Their positions and intensities are given in table 1. The energies of the bands are about 1.9 times higher than those of the three librational levels in the 45–60 meV region. From the fundamental transitions (at 47.1, 50.2 and 55.8 meV), three harmonic overtones (at 94.2, 100.4 and 111.6 meV) and three combinations (at 97.3, 102.9 and 106.0 meV) are predicted. There is no entirely satisfactory correspondence between the harmonic prediction and the observed band positions, although the transition at 90.3 meV is almost certainly the lowest overtone, predicted at 94.2 meV, which has been anharmonically depressed by 3.9 meV.

Allowing for a similar depression of the next overtone ($100.4 - 3.9 = 96.5$ meV) suggests that the 95.3 feature is also an overtone; beyond that however the assignments become confused. The total intensity in the overtone region, S_2, can be compared with the total intensity in the fundamentals, S_1. In the isotropic harmonic approximation (Graham *et al* 1983)

$$\frac{S_n}{S_1} = \frac{1}{n!}\left(\frac{\hbar}{2M\omega_0}\right)^{n-1}\frac{Q_n^{2n}}{Q_1^2}\exp\left\{-\frac{\hbar}{2M\omega_0}(Q_n^2 - Q_1^2)\right\}$$

where $\hbar\omega_0$ is the energy of the ground state, Q_i is the neutron momentum transfer for the energy of the ith level and $M = 4$ amu is the effective mass of the ammonium ion for librations. The calculated ratio S_2/S_1 is 0.42, while the experimental value is 0.21. The disagreement may be attributed to two-phonon scattering of translations and librations, not included in the calculations of Graham *et al* (1983). The present case of NH_4CdF_3 differs from the observation for NH_4Cl (Goyal *et al* 1986), where the harmonic approximation yielded good agreement, probably because the two-phonon contributions did not coincide with the librational overtones.

5.3. The librational spectrum in the low-temperature phase

The low symmetry of the low-temperature phase makes the calculation of the librational energies from an SAF potential difficult. Far more terms are required in this expansion than in the cubic case considered above. Moreover there is a corresponding increase in the number of fitted parameters and a loss of precision. We shall therefore begin by exploring the limitations of the deep-well approximation. Despite the low E_a values of the Zn and Mn salts this approximation retains some utility and provides a simple view of the ammonium ion's librational motions. Initially we avoid the expansion in SAFs, calculate the potential numerically by using point charges (0.42 e^+ on the hydrogens) at the known atomic positions (Rubín *et al* 1995b) and obtain the librational energies in the harmonic approximation.

Table 3. Librational energies, E_{lmn}, of the NH_4^+ ion in NH_4ZnF_3, NH_4MnF_3 and NH_4CdF_3 in the low-temperature phase calculated in the harmonic approximation. The effective charge for the H atom was taken as $f = 0.42e^+$. The indices lmn are the harmonic quantum numbers. E_{Li} are the experimental librational energies. All energies are in meV.

	NH_4ZnF_3	NH_4MnF_3	NH_4CdF_3
E_{L1}	38.7	41.7	47.1
E_{L2}	42.0	44.5	50.2
E_{L3}	45.5	49.0	55.8
E_{010}	17.0	20.0	23.0
E_{001}	18.2	20.7	24.4
E_{100}	23.1	27.0	31.1

The results of this calculation have been collected and compared to the experimental values in table 3. The calculated values of the librational energies are always smaller than experiment, but the calculated relative splitting is 16% larger than the observed one in the whole series. As was seen in the high-temperature results, above, this is probably a reflection of the chosen hydrogen charge. Adjusting this charge accordingly provides a good fit to the librational bands but is an unphysically large value, 0.85 e^+. We believe that this is a consequence of the naivety of the model and the large value reflects other, ignored,

interactions. Alternatively it may be that the ion is significantly deformed away from its ideal tetrahedral symmetry. This would increase its interaction with the closest fluorines but structural studies support no significant ammonium deformation (Rubín *et al* 1995b). From these calculations we identify the lowest-energy libration (of character A′ (Laguna *et al* 1993)) with oscillations about the crystallographic axis *b* (this is a principal axis in all three salts). Perhaps the most significant failing of the deep-well approximation is its inability to explain the intensity distribution. The three librational bands have quite different intensities and this is not understandable in the deep-well approximation. We therefore return to the SAF approach.

The approach will be similar to our analysis of the high-temperature phase above. Here, however, the ammonium ion has C_s symmetry and is on a C_s site (Rubín *et al* 1995b). The direct product group $C_2 \times C_2$ should therefore be used and this would lead to an expansion of the potential energy function with terms V_2 and V_3. We shall explore the true importance of this relatively low symmetry by attempting to treat the problem in a higher-symmetry framework and introduce lower-symmetry terms as they are needed. We begin with an idealized ammonium ion, T_d, on a C_s site. Again the Q_p group for T_d is O, and the corresponding Q_p group of C_s is the proper group C_2 (Miller and Decius 1973). The product group $O \times C_2$ gives rise to an expansion of the potential energy in seven terms up to $J = 6$. We introduce a simplification by ignoring the out-of-phase tilts of the MF_6 octahedra (mode R'_{15}) since they are smaller than the in-phase tilts (mode M_2) (Laguna *et al* 1993). Although the site symmetry is now C_{2v} and the corresponding Q group is D_2, it so happens that both $O \times C_2$ and $O \times D_2$ are identical up to $J = 6$. We choose to underline this here because we shall continue with the product group $O \times D_2$ and introduce a further simplification below. The potential energy function can now be expanded as previously

$$V(\Omega) = B\beta(\beta_{41}V_{41}(\Omega) + \beta_{42}V_{42}(\Omega) + \beta_{43}V_{43}(\Omega) + \beta_{61}V_{61}(\Omega) + \beta_{62}V_{62}(\Omega) + \beta_{63}V_{63}(\Omega) + \beta_{64}V_{64}(\Omega)) \tag{4}$$

where the SAFs $V_{J,n}$ are listed in the appendix.

Now there are eight parameters (β and seven $\beta_{J,n}$ parameters). The correspondence between the $\beta_{J,n}$ parameters in $O \times O$ and $O \times D_4$, and between $O \times D_4$ and $O \times D_2$, is shown in the appendix. There are three parameters in $O \times D_2$ with no correspondence in $O \times D_4$ (β_{42}, β_{62} and β_{64}). These parametrize the in-phase tilt of the MF_6 octahedra and are needed to produce a structure with space group $P4/mbm$ and C_{2v} ammonium site symmetry. Further out-of-phase tilts give the space group $Pnma$ and site symmetry C_s. As a starting point we consider the case of a stretched cube. D_4 is the point group symmetry with only proper rotations of a cube stretched along a fourfold axis. This is the simplest representation of a tetragonal perovskite structure in the low-temperature phase. The cell parameters are retained but the tilts have been suppressed. The three parameters β_{42}, β_{62} and β_{64} are therefore set to zero. The model must predict the INS band positions and intensities in the librational region and, moreover, the E_a of the rotational process observed at higher temperatures in the same phase. However convergence may not have been completed with our limited basis ($L < 12$) and we anticipate discrepancies between the calculated and observed E_a values. Each level is given an intrinsic width, in a similar way to the cubic phase above, and a Debye–Waller factor.

The results of the calculations for the Zn salt are shown in figure 7 alongside the INS spectrum, the parameters are detailed in table 2. Seven parameters were adjusted: β, β_{41}, β_{43}, β_{61}, β_{63}, U^2 and the spectral width (final values $U^2 = 0.04$ Å^2, FWHH = 1.6 meV). The profile of the observed librational spectrum is well reproduced, though the intensity of the central peak, at 42 meV, is somewhat overestimated. The INS intensity around 70 meV

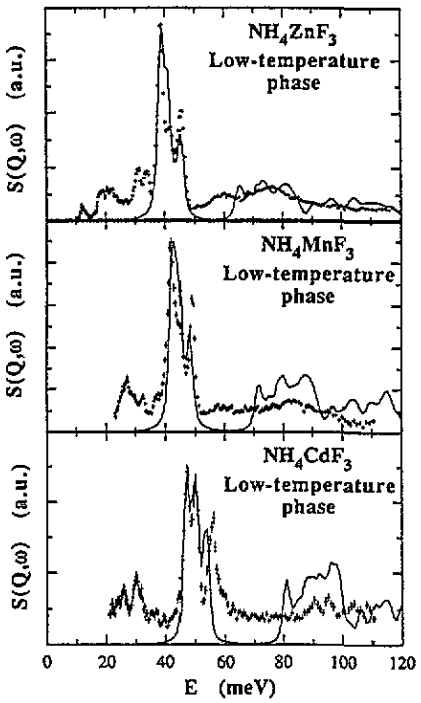

Figure 7. Simulation of the librational INS spectra of the NH_4^+ ion of NH_4ZnF_3, NH_4MnF_3 and NH_4CdF_3 in the low-temperature phase using the calculated energy levels obtained from the potential energy function given by expression (4) and the potential parameters of table 2.

is also outlined. Interestingly the parameters $\beta_{J,n}$ are only slightly different from their, cubic phase, starting values. This is precisely what would be expected for a structural transition involving little atomic dislocation. The parameter β, here fitted to $\beta = 59$, is clearly larger than in the high-temperature phase ($\beta = 50$). If the point charge model is again recalled, this value of β corresponds to an effective charge of $\approx 0.62e^+$. Altogether the agreement is good despite the two drastic approximations: the ammonium ion has T_d symmetry and the crystal has D_4 symmetry.

The quality of the fit to the Zn salt spectrum stems, in part, from the very small tilts of the MF_6 octahedra in this salt. Consequently the main features of the Zn salt's symmetry are well represented by the D_4 model and including small values for parameters β_{42}, β_{62} and β_{64} does not significantly improve the agreement. Indeed any significant value for the parameters, especially for β_{42}, introduces intense features into the calculated spectrum, about 10 meV. We have also investigated the possibility of cancellation effects, where the parameters could have significant values but opposite signs. Again the calculated spectra rapidly deviate from observations, principally in the librational region.

The same calculations for the Mn and Cd salts require small values for β_{62} and β_{64}. Their fits are also shown in figure 7. Here the librational levels were broadened by (FWHH) Mn salt = 1.6 meV and Cd salt = 1 meV and the mean square displacements required for an acceptable fit, U^2, where Mn salt = 0.024 Å^2 and Cd salt = 0.016 Å^2. The calculated spectra of both salts were too intense in the 44.5 meV region and the splitting of the bands in the Cd salt was underestimated. The very fact that β_{62} and β_{64} appear at all implies that the overall symmetry has been reduced to D_2 by the in-phase tilts of the MF_6 octahedra

(about the crystallographic b axis, mode M_2). In the Mn salt the β value is higher in this low-temperature phase, $\beta = 66$, than in the high-temperature phase, $\beta = 54$, which probably reflects the shorter F–H distance. In the Cd salt the very high β value, $\beta = 75$, implies an even shorter F–H distance. However, this value of β amounts to an effective charge of $\approx 0.78e^+$, an unrealistic value which again points to the inadequacy of the electrostatic interactions (proportional to the effective charge) as unique in the atom–atom potential.

Our treatment of the problem by approximating the true point symmetry of the ion by T_d and the crystallographic symmetry by D_4, or D_2, has proved successful. Previously it was thought that the $\beta\beta_3 V_3$ term of the multipole expansion would be more important in the interaction potential (Smith 1994). This is not supported by the INS data. Significant values for the low-symmetry contributions would give an entirely different shape to the INS spectra. Our results are in agreement with recent crystallographic work that shows only slight distortions of the ammonium ion away from ideality (Rubín *et al* 1995b), significantly more ideal than was previously thought (Helmholdt *et al* 1980). An important result then is that although the V_2 and V_3 terms are strictly necessary they are present only as weak perturbations.

The band widths were not extracted directly from the data but, rather, chosen to produce a reasonable spectral resemblance. However, the features of the low-temperature phase are sharper than in the high-temperature phase. This shows that the excited librational states live longer, probably by about an order of magnitude. The band widths, see table 1, are comparable with those obtained from the low-temperature phase Mn salt by Raman spectroscopy, ≈ 1 meV (Rubín *et al* 1995a).

6. Conclusions

We have reported the INS spectra of some ammonium metal fluorides (metal = Zn, Mn, Cd) in both the high-temperature, cubic, phase (Zn and Mn salts) and the low-temperature, tetragonal phase. Whilst the high-temperature spectra show broad weak librational bands the low-temperature spectra clearly showed intense structured librational bands. The translational modes were also assigned.

The librational spectra were calculated from a model of the potential energy function which constrains the rotations of a free ammonium ion. The potential was expanded, to leading terms, in functions which possessed the symmetry of the ion and its crystalline environment, the symmetry adapted functions. For a given rotational constant, B, the overall field strength was given by β, with individual contributions of the functions being controlled by their coefficients, $\beta_{J,n}$. To our knowledge, this is the first time that the librational spectrum has been related to the full librational level scheme far from the harmonic approximation.

In the high-temperature phase the parameters β, β_4 and β_6 are important and their values were extracted from fitting the INS data to the calculation. Results for β_4 and β_6 in the Zn salt were comparable to those obtained previously and allowed an independent estimate of the β parameter, $\beta = 50$. This is higher than previous estimates based upon point charge models, with or without polarization effects. The results from the Mn salt support this conclusion but are not so definitive. Lifetime broadening effects were observed for the first time and the lifetime of the first excited librational state in the Zn salt was estimated to be about 0.1 ps. The activation energy for the reorientational motion of the ion was calculated to be in agreement with previous experimental work.

A naive deep-well model based on point charges was used to calculate the INS spectra of the low-temperature spectra. Only the number of librational bands and other general features

of the spectra were reproduced satisfactorily and the final effective charge distributions were unphysically strong. Again the potentials were expanded in symmetry adapted functions. Here we progressed systematically from a relatively high-symmetry approximation of the structure towards the true symmetry of the low-temperature phase. The absence, in the Zn salt, and the weakness, in the Mn and Cd salts, of the low-symmetry terms showed that the potential is dominated by high-symmetry contributions. These contributions were correlated with the known crystallographic structures of the salts. Compared to its high-temperature value, the field strength parameter, β increased in the low-temperature phase for each salt, in satisfactory agreement with expectation from the activation energies of these systems. The lifetime of the first excited librational states also increased in the low-temperature phase.

Acknowledgments

This work has been supported by the CICYT project PB92-1077. We should also like to thank the EPSRC for access to the ISIS Facility, at the Rutherford Appleton Laboratory, UK, and the hospitality of its staff.

Appendix

In the low-temperature phase of the perovskites the rotational potential function (4) contains the following symmetry adapted functions:

$$V_{41}(\Omega) = \frac{\sqrt{3}}{6}\left[\sqrt{7}D^{(4)}_{-4,0}(\Omega) + \sqrt{5}D^{(4)}_{4,0}(\Omega)\right]$$

$$V_{42}(\Omega) = \frac{\sqrt{3}}{6}\left[\sqrt{\frac{7}{2}}(D^{(4)}_{0,-2}(\Omega) + D^{(4)}_{0,2}(\Omega)) + \frac{\sqrt{5}}{4}(D^{(4)}_{-4,-2}(\Omega) + D^{(4)}_{-4,2}(\Omega) + D^{(4)}_{4,-2}(\Omega) + D^{(4)}_{4,2}(\Omega))\right]$$

$$V_{43}(\Omega) = \frac{\sqrt{3}}{6}\left[\sqrt{\frac{7}{2}}(D^{(4)}_{0,-4}(\Omega) + D^{(4)}_{0,4}(\Omega)) + \frac{\sqrt{5}}{4}(D^{(4)}_{-4,-4}(\Omega) + D^{(4)}_{-4,4}(\Omega) + D^{(4)}_{4,-4}(\Omega) + D^{(4)}_{4,4}(\Omega))\right]$$

$$V_{61}(\Omega) = \frac{\sqrt{13}}{2}\left[\frac{1}{\sqrt{2}}D^{(6)}_{-4,0}(\Omega) - \frac{\sqrt{7}}{4}D^{(6)}_{4,0}(\Omega)\right]$$

$$V_{62}(\Omega) = \frac{\sqrt{13}}{4}\left[(D^{(6)}_{0,-2}(\Omega) + D^{(6)}_{0,2}(\Omega)) + \sqrt{\frac{7}{2}}(D^{(6)}_{-4,-2}(\Omega) + D^{(6)}_{-4,2}(\Omega) + D^{(6)}_{4,-2}(\Omega) + D^{(6)}_{4,2}(\Omega))\right]$$

$$V_{63}(\Omega) = \frac{\sqrt{13}}{4}\left[(D^{(6)}_{0,-4}(\Omega) + D^{(6)}_{0,4}(\Omega)) + \sqrt{\frac{7}{2}}(D^{(6)}_{-4,-4}(\Omega) + D^{(6)}_{-4,4}(\Omega) + D^{(6)}_{4,-4}(\Omega) + D^{(6)}_{4,4}(\Omega))\right]$$

$$V_{64}(\Omega) = \frac{\sqrt{13}}{4}\Big[(D^{(6)}_{0,-6}(\Omega) + D^{(6)}_{0,6}(\Omega)) + \sqrt{\frac{7}{2}}(D^{(6)}_{-4,-6}(\Omega) + D^{(6)}_{-4,6}(\Omega) + D^{(6)}_{4,-6}(\Omega) + D^{(6)}_{4,6}(\Omega))\Big]$$

where $D^{(J)}_{k,m}(\Omega)$ are Wigner functions (we use the convention of Edmonds (1957)). The symmetry of the rotational states which appear in the fundamental and first excited set for the parameters β and $\beta_{J,n}$ used in this paper is indicated in table A1.

Table A1. Irreducible representations of the rotational states in the $O \times D_2$ symmetry potential, where O is the molecule group, M, and D_2 is the site symmetry group, S. Γ_M and Γ_S stand for the irreducible representations of the point groups O and D_2 respectively. The number of states with symmetry $\Gamma_M \times \Gamma_S$ is $N = ng$, where n is the times the states appear and g is the degeneracy of that state. N is given for the fundamental and first excited set of levels calculated with the β parameters in used in the text.

$\Gamma_M \times \Gamma_S$	Degeneracy	N (fundamental set)	N (excited set)
$A_1 \times A_1$	5	15	0
$A_1 \times B_1$	5	0	15
$A_1 \times B_2$	5	0	15
$A_2 \times B_3$	5	0	15
$A_2 \times A_1$	5	0	15
$A_2 \times B_1$	5	5	10
$A_2 \times B_2$	5	5	10
$A_2 \times B_3$	5	5	10
$E \times A_1$	2	6	6
$E \times B_1$	2	2	10
$E \times B_2$	2	2	10
$E \times B_3$	2	2	10
$T_1 \times A_1$	3	0	27
$T_1 \times B_1$	3	9	18
$T_1 \times B_2$	3	9	18
$T_1 \times B_3$	3	9	18
$T_2 \times A_1$	3	9	18
$T_2 \times B_1$	3	6	21
$T_2 \times B_2$	3	6	21
$T_2 \times B_3$	3	6	21
Total number of states		96	288

The case $O \times D_2$ (expression (4)) includes that of $O \times D_4$ (Burriel *et al* 1981) and $O \times O$ (Bartolomé *et al* 1977). The expansion of the case $O \times O$ is given in expression (3), while that of $O \times D_4$ is

$$V(\Omega) = B\beta(\beta_{41}V_{41}(\Omega) + \beta_{42}V_{42}(\Omega) + \beta_{61}V_{61}(\Omega) + \beta_{62}V_{62}(\Omega)).$$

The corresponding SAFs are related to those of the case $O \times D_2$ as

$$V_{41}(O \times D_4) = D_{41}(O \times D_2)$$
$$V_{42}(O \times D_4) = V_{43}(O \times D_2)$$
$$V_{61}(O \times D_4) = V_{61}(O \times D_2)$$
$$V_{62}(O \times D_4) = V_{63}(O \times D_2)$$
$$V_4(O \times O) = \frac{1}{2}\sqrt{\frac{7}{3}}V_{41}(O \times D_4) + \frac{1}{2}\sqrt{\frac{5}{3}}V_{42}(O \times D_4)$$

$$V_6(O \times O) = \frac{1}{2\sqrt{2}} V_{61}(O \times D_4) - \frac{1}{2}\sqrt{\frac{7}{2}} V_{62}(O \times D_4)$$

which leads to the following relationship between the parameters $\beta_{J,n}$

$$\beta_{41}(O \times D_2) = \beta_{41}(O \times D_4) = \frac{1}{2}\sqrt{\frac{7}{3}}\beta_4(O \times O)$$

$$\beta_{43}(O \times D_2) = \beta_{42}(O \times D_4) = \frac{1}{2}\sqrt{\frac{5}{3}}\beta_4(O \times O)$$

$$\beta_{61}(O \times D_2) = \beta_{61}(O \times D_4) = \frac{1}{2\sqrt{2}}\beta_6(O \times O)$$

$$\beta_{63}(O \times D_2) = \beta_{62}(O \times D_4) = -\frac{1}{2}\sqrt{\frac{7}{2}}\beta_6(O \times O)$$

while $\beta_{42}(O \times D_2)$ and $\beta_{62}(O \times D_2)$ are independent of those of the higher symmetries.

References

Agulló-Rueda F, Calleja J M and Bartolomé J 1988 *J. Phys. C: Solid State Phys.* **21** 1287

Altmann S L and Cracknell A P 1965 *Rev. Mod. Phys.* **37** 19

Bartolomé J, Navarro R, González D and de Jongh L J 1977 *Physica* B **92** 45

Bartolomé J, Palacio F, Calleja J M, Agulló Rueda F, Cardona M and Migoni R 1985 *J. Phys. C: Solid State Phys.* **18** 6083

Bradley C J and Cracknell A P 1972 *The Mathematical Theory of Symmetry in Solids* (Oxford: Clarendon)

Brom H B and Bartolomé J 1981 *Physica* B **111** 183

Burriel R, Bartolomé J, Navarro R and González D 1981 *Recent Developments in Condensed Matter Physics* vol 4, ed J T Devreese, L F Lemmees, V E van Doren and J van Royen (New York: Plenum) pp 1–10

Edmonds A R 1957 *Angular Momentum in Quantum Mechanics* (Princeton, NJ: Princeton University Press)

Gerling R W and Hüller A 1983 *J. Chem. Phys.* **78** 446

Goyal P S, Boland B C, Penfold J, Taylor A D and Tomkinson J 1987 *Dynamics of Molecular Crystals* (Amsterdam: Elsevier) p 429

Goyal P S, Penfold J and Tomkinson J 1986 *Chem. Phys. Lett.* **127** 483

Graham D, Howard J, Waddington T C and Tomkinson J 1983 *J. Chem. Soc., Faraday Trans.* II **79** 1713

Helmholdt R B, Wiegers G A and Bartolomé J 1980 *J. Phys. C: Solid State Phys.* **13** 5081

King H F and Hornig D F 1966 *Can. J. Chem.* **44** 4520

Knop O, Oxton I A, Westerhaus W J and Falk M 1981 *J. Chem. Soc., Faraday Trans.* II **77** 309

Laguna M A, Sanjuán M L, Orera V M, Rubín J, Palacios E, Piqué M C, Bartolomé J and Berar J F 1993 *J. Phys.: Condens. Matter* **5** 283

Le Bail A, Fourquet J L, Rubín J, Palacios E and Bartolomé J 1990 *Physica* B **162** 231

Miller R E and Decius J C 1973 *J. Chem. Phys.* **59** 4871

Otnes K and Svare I 1979 *J. Phys. C: Solid State Phys.* **12** 3899

Ozaki Y, Maki K, Okada K and Morrison A 1985 *J. Phys. Soc. Japan* **54** 2595

Palacios E, Bartolomé J, Burriel R and Brom H B 1989 *J. Phys.: Condens. Matter* **1** 1119

Penfold J and Tomkinson J 1986 *RAL Report* RAL86019

Powell B M, Press W and Dolling G 1985 *Phys. Rev.* B **32** 3118

Prager M, Press W, Alefeld B and Hüller A 1977 *J. Chem. Phys.* **67** 5126

Press W and Hüller A 1973 *Acta Crystallogr.* A **29** 252

Rubín J, Bartolomé J, Anne M, Kearley G J and Magerl A 1994 *J. Phys.: Condens. Matter* **6** 8449

Rubín J, Bartolomé J, Laguna M A and Sanjuán M L 1995a *Physica* B at press

Rubín J, Palacios E, Bartolomé J and Rodríguez-Carvajal J 1995b *J. Phys.: Condens. Matter* **7** 563

Smith D 1987 *J. Chem. Phys.* **86** 4055

——1994 *Chem. Rev.* **94** 1567

Steenbergen Chr, de Graaf L A, Bevaart L, Bartolomé J and de Jongh L J 1979 *J. Chem. Phys.* **70** 1450

Teh H C and Brockhouse B N 1971 *Phys. Rev.* **83** 2733

Venkataraman G and Sahni V C 1970 *Rev. Mod. Phys.* **42** 409